Introduction to the inverse kinematics of serial manipulators

Sandipan Bandyopadhyay
Department of Engineering Design
Indian Institute of Technology Madras, Chennai 600 036
Email: sandipan@iitm.ac.in
Web: http://www.ed.iitm.ac.in/~sandipan

1 Introduction

Position analysis is an essential step in the design, analysis and control of robots. In this article, a basic introduction to the position analysis of serial manipulators is given. This topic is invariably covered in all the textbooks on this subject. Therefore, instead of repeating the standard details of forward kinematics, such as, the designation of the reference frames, determination of the Denavit-Hartenberg (DH) parameters, multiplication of the 4×4 transformation matrices to get the end-effector position and orientation etc., more emphasis is laid on the inverse problem, which is relatively more complicated in such manipulators. Simple examples, such as a planar 2-R and a spatial 3-R serial robot are discussed in detail. Related concepts, including the numbers of solutions to the inverse kinematic problem, condition(s) for coincidence of the solution branches and their equivalence with singularities, the workspace boundaries as the loci of singular configurations etc. are presented in a manner that once the reader follows these clearly, he/she would find it very easy to apply these to another manipulator. Multiple approaches to the same problem are included to provide just a fleeting glance at the richness of this fascinating subject, and to suit the potentially different tastes of the readers.

As the reader is expected to be familiar with the basic concepts, the rest of the article would focus more on the actual solution of two representative examples, one planar and

another spatial. For further details, the reader is directed to the standard texts in this domain [1, 2, 3].

2 Example 1: 2-R planar manipulator

Let us consider one of the simplest possible manipulators in this section, namely, the 2-R planar serial robot. The robot is shown in Fig. 1. The designation "2-R" derives from the

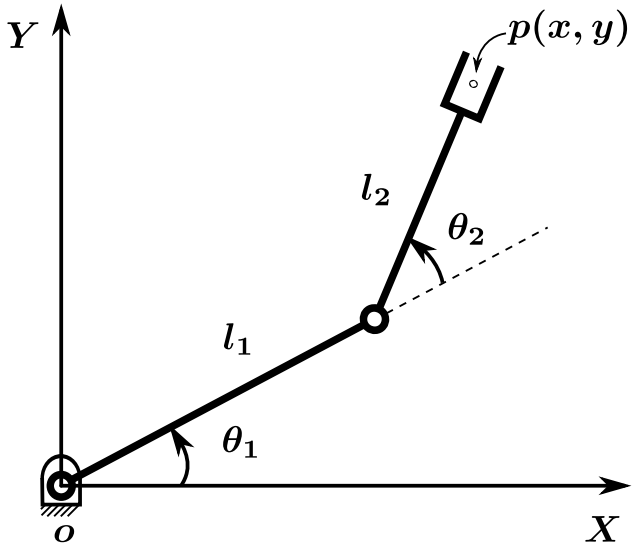

Figure 1: Schematic of the 2-R planar serial robot

fact that the robot has one rotary actuator (i.e., motor) at each of its joints. The problem of position kinematics (also known as *zeroth-order kinematics*) can be further divided in two subproblems: *forward*, and *inverse* kinematics. These are discussed in the following.

2.1 Forward kinematics of the planar 2-R manipulator

Forward kinematics refers to the problem of finding the position of the *end-effector* (in this case, represented by the point $\boldsymbol{p} = (x, y)^T$ in Fig. 1), given the link lengths l_1, l_2, and the *inputs* $\boldsymbol{\theta} = (\theta_1, \theta_2)^T$. For this manipulator, the forward kinematics problem is trivially solved by observing Fig. 1:

$$x = l_1 \cos\theta_1 + l_2 \cos\theta_{12}, \tag{1}$$

$$y = l_1 \sin\theta_1 + l_2 \sin\theta_{12}, \quad \text{where } \theta_{12} = \theta_1 + \theta_2. \tag{2}$$

Eqs. (1,2) are also referred to as the *forward kinematic map*[1], as they map the joint angles $(\theta_1, \theta_2)^T$ to the tip coordinates $(x, y)^T$. As this map is nonlinear in nature, the *inverse* of it, i.e., finding the *inverse kinematic map*, is generally more complicated.

2.2 Inverse kinematics of the planar 2-R manipulator

As explained above, the task in this case is to find θ_1, θ_2, given x, y. There are multiple ways of solving this problem, and some of these are noted below.

2.2.1 Trigonometric method

Note that Eqs. (1,2) are nonlinear in θ_1, θ_2, but these are *linear* in the sines and cosines of θ_1, θ_{12}. Taking advantage of this, we solve for $\cos\theta_1, \sin\theta_1$:

$$\cos\theta_1 = (x - l_2\cos\theta_{12})/l_1 \tag{3}$$

$$\sin\theta_1 = (y - l_2\sin\theta_{12})/l_1; \quad l_1 > 0. \tag{4}$$

In the above, the sine and cosine of θ_1 have been taken to be two distinct unknown variables. Obviously, to complete the solution meaningfully, we need to state the inherent dependence of these two explicitly:

$$\cos^2\theta_1 + \sin^2\theta_1 - 1 = 0. \tag{5}$$

After performing some simplifications, Eq. (5) reduces to the following form:

$$a\cos\theta_{12} + b\sin\theta_{12} + c = 0, \quad \text{where} \tag{6}$$

$$a = 2l_2x, b = 2l_2y, c = l_1^2 - l_2^2 - x^2 - y^2. \tag{7}$$

The manipulations stated above serve one key purpose: they reduce a pair of *simultaneous* equations in θ_1, θ_{12} to a single equation (6) in a single unknown θ_{12}. However, this equation requires further processing, so that it can be *solved trigonometrically*. Recall that it is possible to directly solve only three classes of equations (and their reciprocals) in trigonometry:

$$\cos\phi = d, \tag{8}$$

$$\sin\phi = e, \tag{9}$$

$$\tan\phi = f, \quad \text{where } d, e \in [-1, 1];\ f, \phi \in \mathbb{R}. \tag{10}$$

[1]It is interesting to note here that the said map is not from $\mathbb{R}^2$ to $\mathbb{R}^2$, as it might seem on the surface. If it is assumed that both the joints allow *full-cycle mobility*, i.e., there is no physical limit on the joint motions, then $\theta_1, \theta_2 \in \mathbb{S}^1$, and thus $(\theta_1, \theta_2)^T \in \mathbb{T}^2 \equiv \mathbb{S}^1 \times \mathbb{S}^1$.

Therefore, Eq. (6) needs to be transformed to one of these *solvable* forms. Let us start with the following step:

$$\frac{a}{\sqrt{a^2+b^2}}\cos\theta_{12} + \frac{b}{\sqrt{a^2+b^2}}\sin\theta_{12} + \frac{c}{\sqrt{a^2+b^2}} = 0, \quad \text{assuming } a^2+b^2 > 0. \tag{11}$$

Further, as seen in Fig. 2, $\frac{a}{\sqrt{a^2+b^2}} = \cos\psi$ and $\frac{b}{\sqrt{a^2+b^2}} = \sin\psi$, for some angle ψ, determined

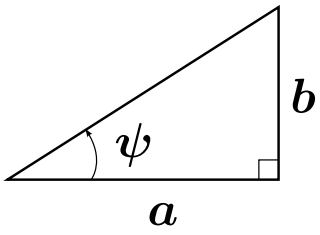

Figure 2: Geometric interpretation of the angle ψ

uniquely by:

$$\psi = \arctan(b, a), \tag{12}$$

where $\arctan(\sin(\cdot), \cos(\cdot))$ represents the *two-argument arctangent function*[2]. With these, Eq. (11) reduces to:

$$\cos\psi\cos\theta_{12} + \sin\psi\sin\theta_{12} = -\frac{c}{\sqrt{a^2+b^2}} \tag{13}$$

$$\Rightarrow \cos(\theta_{12}-\psi) = -\frac{c}{\sqrt{a^2+b^2}}, \quad \text{assuming } a^2+b^2 > 0. \tag{14}$$

For the above equation to have a real solution in the remaining unknown θ_{12}, we must ensure:

$$\left|\frac{-c}{\sqrt{a^2+b^2}}\right| \in [0,1]$$

$$\Rightarrow a^2+b^2-c^2 \geq 0 \tag{15}$$

If this condition holds good, then we get:

$$\theta_{12} - \psi = \pm\arccos\left(\frac{-c}{\sqrt{a^2+b^2}}\right) \tag{16}$$

$$\Rightarrow \theta_{12} = \pm\arccos\left(\frac{-c}{\sqrt{a^2+b^2}}\right) + \arctan(b,a). \tag{17}$$

[2]The need for such a function as opposed to the "common" single-argument version of it is explained in Appendix A.

Thus, there are *two* solutions for θ_{12} for a given x, y, under the above assumptions.For each of these solutions, the corresponding values of θ_1 can be computed from Eqs. (3,4) as:

$$\theta_1 = \arctan(y - l_2 \sin\theta_{12}, x - l_2 \cos\theta_{12}) \tag{18}$$

These two distinct pairs of solutions are also known as the *branches* of inverse kinematics.

This completes the solution of the inverse kinematic problem, in the *general* case. Let us now take a look at the *special cases*, in particular, when $a^2 + b^2 - c^2 = 0$.

After substituting the expressions for a, b, c from Eq. (7) into Eq. (15) and performing some simplifications, this condition reduces to:

$$(x^2 + y^2 - (l_1 - l_2)^2)(x^2 + y^2 - (l_1 + l_2)^2) = 0 \tag{19}$$

It can be seen that condition (19) holds true on the two solid circles shown in Fig. 3. These

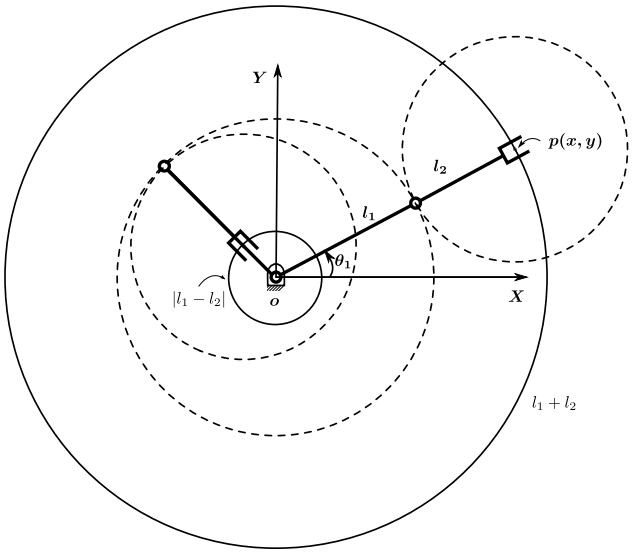

Figure 3: Singularities and workspace of the planar 2-R manipulator

circles delimit the set of points in the plane that the manipulator can "reach". In other words, these circles define the boundaries of the *workspace* (or more precisely, the *reachable workspace*) of the manipulator. The reader can readily verify from Eq. (16) the collapse of the two branches of the solutions of inverse kinematics to *one* in this case – a phenomenon also called as a *singularity*. Much more on this can be found in the standard textbooks [1, 2, 3]. Finally, it should be obvious as to what happens when condition (15) is violated. If not, the reader can find more about it below.

2.2.2 Algebraic method

Methods from algebraic geometry are very popular in the study of position kinematics of robot manipulators. There is a reasonable introduction to the topic in [2], and the references therein. While these methods can be very powerful, they generally require *symbolic manipulations*, i.e., the use of *computer algebra systems* (CAS) such as `Maple`, `Mathematica`, `Singular`, etc. As the scope of discussion in this article is very limited, only the treatment of a single equation would be shown here. The reader can refer to [4] for acquiring the theoretical background in solving systems of multi-variate equations, and find some applications of these in robotics in [2].

Let us pick up the analysis again at Eq. (6), i.e., after the variable θ_1 has been *eliminated*, leaving behind a *univariate* equation in θ_{12}. It is well-known, that such an equation can be converted into a *polynomial* equation in a single algebraic variable. This is achieved by the use of two trigonometric identities:

$$\cos\theta_{12} = \frac{1-t^2}{1+t^2},\ \sin\theta_{12} = \frac{2t}{1+t^2}, \quad \text{where } t = \tan(\theta_{12}/2). \tag{20}$$

Substituting these in Eq. (6), we get after some rationalisation and collection of *like* terms:

$$(c-a)t^2 + 2bt + (c+a) = 0 \tag{21}$$

Some of the observations made in Section 2.2.1 are obvious from Eq. (21). For instance, it is obvious that there are two solutions to the problem in the general case. To investigate the special cases, let us now study the *discriminant* of the quadratic equation:

$$\Delta = 4(a^2 + b^2 - c^2). \tag{22}$$

The condition for having two *distinct* real roots is that $\Delta > 0$. It should not be surprising that this is identical to the condition for the *general* case described in Section 2.2.1. Likewise, $\Delta = 0$ implies a *repeated real root*, and $\Delta < 0$ results in a *pair of complex conjugate roots*, indicating that the commanded position for the end-effector $\boldsymbol{p}(x, y)$ is beyond the reach of the manipulator, i.e., *outside its workspace*. Thus, physically meaningful solutions are obtained only in the cases $\Delta \geq 0$. From the solutions of Eq. (21) the unknown θ_{12} can be solved for as:

$$\theta_{12} = 2\arctan(t). \tag{23}$$

Why the single argument version of arc-tangent function works in this case as opposed to the two-argument version of it is explained in Appendix B.

2.2.3 Geometric method

Consider posing the inverse kinematic problem in a different way, which does not use the forward kinematic equations as a starting point. In Fig. 1, there are two *known points*:

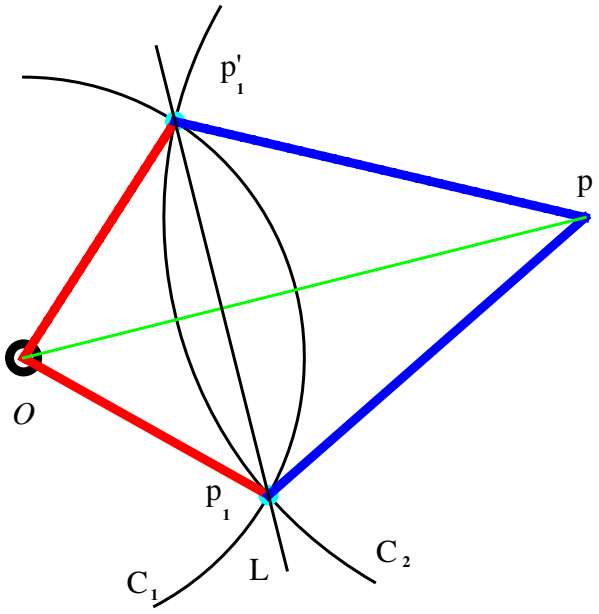

Figure 4: Geometric interpretation of the two branches of inverse kinematics of the 2-R serial manipulator

the origin $\boldsymbol{O}$, and the tip point $\boldsymbol{p}$. The point $\boldsymbol{p}_1$, being the tip of link 1, is constrained to lie on the circle C_1. Likewise, $\boldsymbol{p}_1$ also lies on the circle C_2, being an end point of link 2. Therefore, the locus of the point $\boldsymbol{p}_1(x_1, y_1)$ is confined to the intersections of the circles C_1, C_2. This is depicted in Fig. 4, where the two branches of inverse kinematics are shown as $\boldsymbol{O}$-$\boldsymbol{p}_1$-$\boldsymbol{p}$ and $\boldsymbol{O}$-$\boldsymbol{p}'_1$-$\boldsymbol{p}$ respectively. As the 2-R is similar to the human hand in architecture, these configurations are generally termed as "elbow-down" and "elbow-up" respectively, the point $\boldsymbol{p}_1$ (equivalently, $\boldsymbol{p}'_1$) being the "elbow". The mathematical steps for finding the two configurations follow. The equations of the circles C_1, C_2 are given by, respectively:

$$x_1^2 + y_1^2 - l_1^2 = 0 \tag{24}$$

$$x_1^2 + y_1^2 + x^2 + y^2 - 2xx_1 - 2yy_1 - l_2^2 = 0 \tag{25}$$

Deducting Eq. (25) from Eq. (24), we get a linear equation in x, y, which describes the common chord L of the two circles passing through the points $\boldsymbol{p}_1, \boldsymbol{p}'_1$:

$$2xx_1 + 2yy_1 - x^2 - y^2 + l_2^2 - l_1^2 = 0. \tag{26}$$

Solving Eq. (26) for y_1, we get:

$$y_1 = \frac{l_1^2 - l_2^2 + x^2 + y^2 - 2xx_1}{2y}, \quad \text{assuming } y \neq 0. \tag{27}$$

Substituting the expression for y in the equation of one of the circles, say, C_1, we get a quadratic equation in x_1:

$$\begin{aligned} &a_1 x_1^2 + b_1 x_1 + c_1 = 0, \quad \text{where} \\ &a_1 = 4(x^2 + y^2),\ b_1 = -4x(l_1^2 - l_2^2 + x^2 + y^2), \\ &c_1 = (x^2 + y^2)^2 + l_1^4 - 2l_1^2 l_2^2 + l_2^4 + 2l_1^2 x^2 - 2l_2^2 x^2 - 2l_1^2 y^2 - 2l_2^2 y^2. \end{aligned} \tag{28}$$

All the results obtained in the other methods, i.e., number of solutions, singularity conditions etc., can also be derived in this method as well. In addition, another geometric condition for singularity emerges from this analysis. At a singularity, the circles C_1, C_2 are tangential to each other, the point of tangency being $\boldsymbol{p}_1$, (which coincides with $\boldsymbol{p}_1'$ in this configuration). Equivalently, the common chord becomes the common tangent. The reader is encouraged to draw the singular configurations to validate the above surmises.

3 Example 2: 3-R spatial manipulator

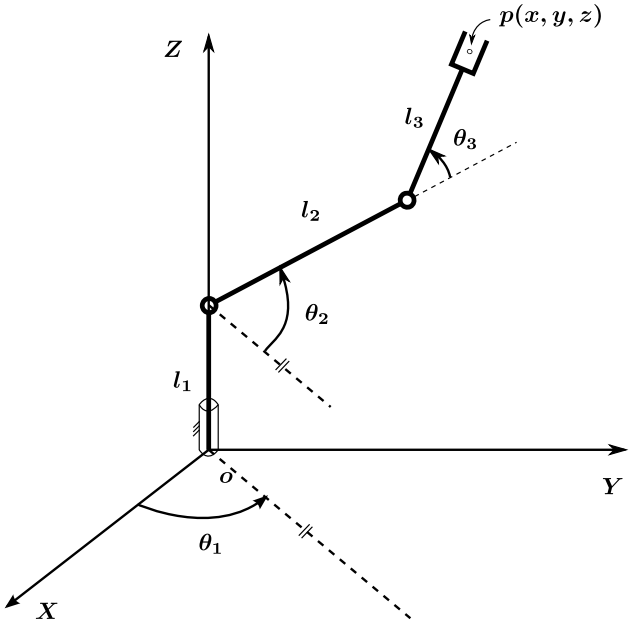

Figure 5: Schematic of the 3-R spatial manipulator

Let us now consider a simple spatial manipulator, namely, the spatial 3-R. The robot is shown schematically in Fig. 5. In spite of the simplicity, the architecture of this manipulator

is important for one reason: it captures the general design of the first three joints and links of many *wrist-decoupled* 6-degrees-of-freedom (6-DoF) industrial manipulators, such as the PUMA, Kuka, Fanuc etc[3]. In other words, such 6-DoF manipulators can be designed by adding a 3-DoF *wrist* at the point $\boldsymbol{p}$ of the 3-R spatial.

3.1 Forward kinematics of the 3-R spatial manipulator

As in the case of the planar 2-R manipulator, the forward kinematics is fairly trivial. The reader can find out the DH parameters of the robot, and perform the forward kinematics in a systematic manner to verify the final results given below:

$$x = \cos\theta_1(l_2\cos\theta_2 + l_3\cos\theta_{23}) \tag{29}$$

$$y = \sin\theta_1(l_2\cos\theta_2 + l_3\cos\theta_{23}) \tag{30}$$

$$z = l_1 + l_2\sin\theta_2 + l_3\sin\theta_{23}, \quad \text{where } \theta_{23} = \theta_2 + \theta_3. \tag{31}$$

3.2 Inverse kinematics of the 3-R spatial manipulator

In this case, there are three unknown inputs: $\boldsymbol{\theta} = (\theta_1, \theta_2, \theta_3)^T$. The position vector of the end-effector, $\boldsymbol{p} = (x, y, z)^T$, is known.

In Eqs. (29,30,31), it can be observed easily that the variable θ_1 appears only in the first two, and that these equations are, once again, linear in the sine and cosine of the angle θ_1. Therefore, the same procedure is adopted to solve for the variable θ_1 (in terms of the other variables) and to eliminate it from the system of equations, resulting in the following equations:

$$\theta_1 = \arctan(y/r, x/r), \quad \text{where } r = \pm\sqrt{x^2 + y^2} \text{ is assumed to be non-zero;} \tag{32}$$

$$l_2\cos\theta_2 + l_3\cos\theta_{23} - r = 0. \tag{33}$$

The two equations, (31, 33) are *simultaneous linear equations* in the sines and cosines of the angles θ_2, θ_{23}. As such, we treat these equations just as above, to solve for, and eliminate one of the two variables, to finally arrive at a univariate equation – which is our eventual objective.

[3]Readers interested in the inverse kinematics of these 6-DoF manipulators may refer to a standard text-book, e.g., [2].

Choosing to solve for θ_2 first, we get:

$$\theta_2 = \arctan(z - l_1 - l_3 \sin\theta_{23}), r - l_3 \cos\theta_{23}), \quad \text{and} \tag{34}$$

$$2l_3 r \cos\theta_{23} + 2l_3(z - l_1)\sin\theta_{23} - r^2 + l_2^2 - l_3^2 - (z - l_1)^2 = 0 \tag{35}$$

We have already seen how to solve equations such as (35) in Section 2.2.1. Solving it, we get real and distinct solutions when the point $\boldsymbol{p}$ is inside the workspace, a repeated real root when the point is on the boundary of the workspace (i.e., when the manipulator is singular), and a pair of complex conjugates when $\boldsymbol{p}$ is outside the workspace. Following the 2-R example, the reader can easily derive the conditions for the singularities and boundaries of the workspace. It is obvious that one of these conditions is already known, since the links 2, 3 form a planar 2-R in the *vertical* plane. Naturally, this condition is independent of the angle θ_1. The reader can verify easily that the other condition is also independent of θ_1. Understanding why it is so is left as an exercise for the reader. The reader is also encouraged to draw the workspace boundaries, as well as the singular configurations of the manipulator for greater understanding of these concepts.

4 Summary

In this brief article, emphasis is laid on the actual computation of forward and more importantly, inverse kinematics of serial robots. Detailed theoretical treatment of these topics are available in many textbooks, some of which have been mentioned in the references. It is hoped that the illustrative examples and the focus on the underlying trigonometric, algebraic, and geometric concepts would nicely complement the basic theories offered in these books. Treatment of more complicated manipulators, e.g., 6-DoF robots such as the PUMA 560, is beyond the scope of the present discussion. However, understanding the concepts described in this article should help the reader to follow the analysis of such manipulators.

References

[1] J. J. Craig, *Introduction to Robotics: Mechanics and Control*. California: Addison Wesley, second ed., 1986.

[2] A. Ghosal, *Robotics: Fundamental Concepts and Analysis*. New Delhi: Oxford University Press, 2006.

[3] S. K. Saha, *Introduction to Robotics*. New Delhi: Tata McGraw-Hill, 2008.

[4] D. Cox, J. Little, and D. O'Shea, *Ideals, Varieties, and Algorithms: An Introduction to Computational Algebraic Geometry and Commutative Algebra*. New York: Springer-Verlag, 1991.

A The two-argument arctangent function

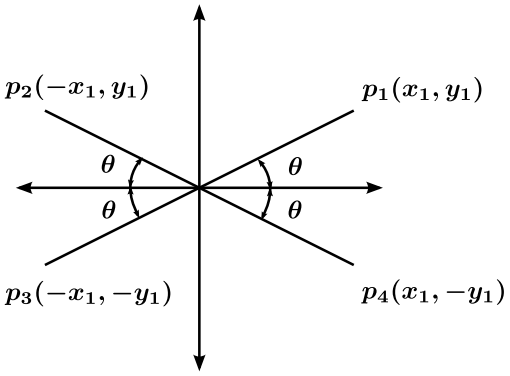

Figure 6: The utility of the $\arctan(\sin(\cdot), \cos(\cdot))$ function

Fig. 6 illustrates why $\arcsin(\cdot), \arccos(\cdot)$, or even $\arctan(\cdot)$ were not used in this article instead of $\arctan(\sin(\cdot), \cos(\cdot))$. Clearly, arcsin fails to distinguish between points $\boldsymbol{p}_1, \boldsymbol{p}_2$, arccos between $\boldsymbol{p}_1, \boldsymbol{p}_4$, and arctan between $\boldsymbol{p}_1, \boldsymbol{p}_3$, while $\arctan(\sin(\cdot), \cos(\cdot))$ alone identifies each point distinctly.

B Bijectivity of the tangent-half-angle function

As seen in Fig. 7, the function $\tan(\alpha/2)$ is *bijective* in the range $\alpha \in [-\pi, \pi]$. Thus, if $t_\alpha = \tan(\alpha/2)$, then $\alpha = 2\arctan(t_\alpha)$ always returns an unambiguous result.

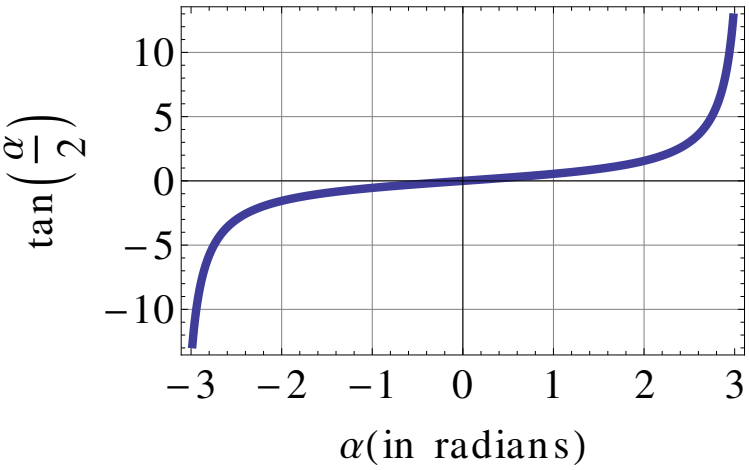

Figure 7: The plot of $\tan(\alpha/2)$ vs. $\alpha \in [-\pi, \pi]$